On dynamics of seismicity simulated by the models of blocks-and-faults systems

Alexandre I. Gorshkov, Vladimir I. Keilis-Borok, Irina M. Rotwain, Alexandre A. Soloviev and Inessa A. Vorobieva
International Institute of Earthquake Prediction Theory and Mathematical Geophysics, Russian Academy of Sciences, Moscow, Russia

Abstract
The major results obtained by numerical simulation of block structure dynamics are juxtaposed and analysed: the possibilities to reconstruct tectonic driving forces from territorial distribution of seismicity, clustering of earthquakes in the model, and dependence of the occurrence of strong earthquakes on fragmentation of the media, and on rotation of blocks. These results show that modelling of block structure dynamics is a useful tool to study relations between the geometry of faults and block movements and earthquake flow, including premonitory seismicity patterns, to test the existing earthquake prediction algorithms, and to develop new ones.

Key words *block structure dynamics – Gutenberg-Richter law – earthquake prediction*

1. Introduction

Caputo *et al.* (1973, 1974, 1980), and Keilis-Borok and Malinovskaya (1964) initiated the study of intermediate-term premonitory seismicity patterns, reflecting respectively, earthquake clustering and increased seismic activity in the medium magnitude range. This was followed by development of a family of earthquake prediction algorithms, their review is given in Keilis-Borok (1990, 1996).

One of the manifestations of premonitory clustering (burst of aftershocks) was the first earthquake precursor, for which statistical significance was rigorously established (Molchan *et al.*, 1990). For other prediction algorithms it was recently confirmed, on basis of long tests by advance prediction (Rotwain and Novikova, 1997; Vorobieva, 1997).

The broad set of premonitory seismicity patterns considered in these algorithms, reflects transformation of the basic features of the dynamics of seismicity (Rotwain *et al.*, 1997): clustering of earthquakes; change of the Gutenberg-Richter (G-R) relation in favour of relatively strong earthquakes, and, probably an increase in the range of correlation of the earthquakes.

These characteristics, however, depend generally speaking not only on the proximity of a strong earthquake, but also on the major properties of seismically active regions. The latter factor was partially eliminated in previous studies by normalization of earthquake flow. Modelling of the dynamics of seismicity in a

Mailing address: Dr. Alexandre A. Soloviev, International Institute for Earthquake Prediction Theory and Mathematical Geophysics, Warshavskoye sh. 79, kor. 2, Moscow 113556, Russia; e-mail: soloviev@mitp.rssi.ru

block and fault system, with realistic geometry, explores regional variations of premonitory phenomena. A synthetic catalog obtained by numerical modelling can cover very long time intervals, thus allowing more reliable identification of these events. From a broader point of view, the dependence in question may allow observed seismicity to be interpreted in terms of internal, directly unobservable features of an earthquake-generating region which are known in the model.

The block models of the lithosphere dynamics were developed and applied to seismicity studies during recent years (Gabrielov *et al.*, 1990, 1994; Soloviev, 1995; Panza *et al.*, 1997; Keilis-Borok *et al.*, 1997).

A seismic region is modelled by a system of absolutely rigid blocks divided by infinitely thin plane faults. The blocks interact between themselves and with the underlying medium. The system of blocks moves as a consequence of prescribed motion of the boundary blocks and of the underlying medium.

As the blocks are absolutely rigid, all deformation takes place in the fault zones and at the block base in contact with the underlying medium. Relative block displacements take place along the fault zones. This assumption is justified by the fact that for the lithosphere the effective elastic moduli of the fault zones are significantly smaller than those within the blocks. Block motion is defined so that the system is in a quasistatic equilibrium state.

The interaction of blocks along the fault zones is viscous-elastic («normal state») while the ratio of the stress to the pressure remains below a certain strength level. When the critical level is exceeded in some part of a fault zone, a stress-drop («failure») occurs (in accordance with the dry friction model), possibly causing failure in other parts of the fault zones. These failures produce earthquakes. Immediately after the earthquake and for some time afterwards, the affected parts of the fault zones are in a state of creep. This state differs from the normal state because of a faster growth of inelastic displacements, lasting until the stress falls below some other level. This numerical simulation gives rise a synthetic earthquake catalog.

Here we juxtapose and analyse the major results of the model: the possibilities to reconstruct tectonic driving forces from territorial distribution of seismicity, clustering of earthquakes in the model, and dependence of the occurrence of strong earthquakes on fragmentation of the media, and on rotation of blocks.

2. Description of the model

The model is described in detail by Gabrielov *et al.* (1990, 1994), Soloviev (1995) and Panza *et al.* (1997). Its brief description is given below.

2.1. *Block structure geometry*

A block structure is a limited and simply-connected part of a layer with thickness H bounded by two horizontal planes (fig. 1). The lateral boundaries of the block structure and its division into blocks are formed by the portions of planes intersecting the layer called «fault zones». The intersection lines of these planes with the upper plane are called «faults». The fault zones have arbitrary dip angles. A common point of two faults is called «the vertex» (three or more faults cannot have a common point on the upper plane). The fault zones intersect with the lower plane and thus in the lower plane there are faults and vertices corresponding to those in the upper plane. The vertex on the upper plane is connected with the corresponding vertex on the lower plane by a segment («rib») of the intersection line of the corresponding fault zones. The part of a fault zone between two ribs corresponding to successive vertices on the fault is called «the fault segment». The shape of the fault segment is a trapezium. The upper and lower surfaces of the blocks are polygons. The lower surface of the block is called «the bottom».

The block structure is bordered by a confining medium. The motion of the confining medium is prescribed in the continuous parts of the block structure boundary, delimited by two ribs. These parts of the confining medium are called «boundary blocks».

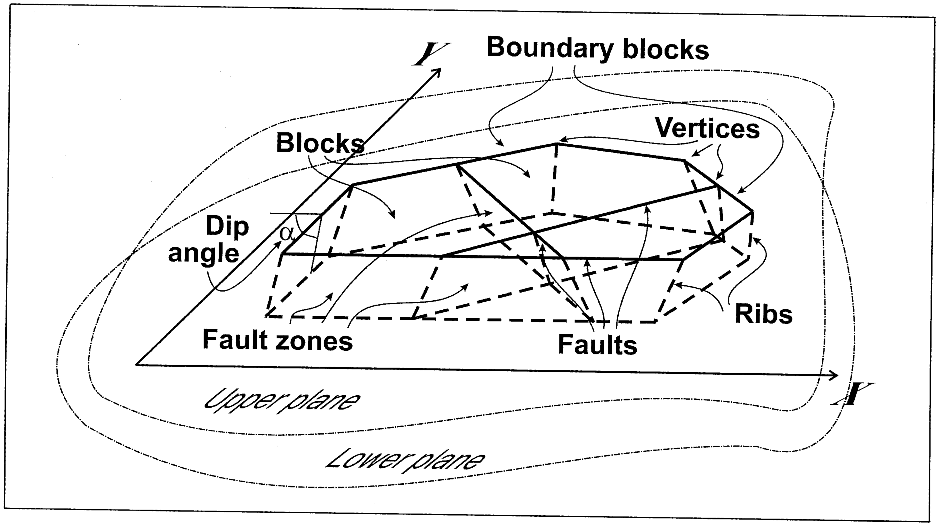

Fig. 1. Definitions used in the block structure model.

2.2. *Movements*

The movements of the boundaries of the block structure (the boundary blocks) and the medium underlying the blocks are assumed to be an external force acting on the structure. The rates of these movements are considered to be horizontal and known. The movement of the underlying medium is specified separately for different blocks.

Non-dimensional time is used in the model, and all quantities containing time are referred to one unit of the non-dimensional time.

At each time the displacements of the blocks are determined in such a way that the structure is in a quasistatic equilibrium. The displacements are supposed to be infinitely small, compared with the block size. Therefore the geometry of the block structure does not change during the simulation and the structure does not move as a whole.

2.3. *Interactions*

The blocks interact with each other along the fault zones separating them and with the underlying medium along the lower plane. This interaction is viscous-elastic.

The elastic stress, due to the displacement of the block relative to the underlying medium, is assumed to be linearly dependent on the difference between the total relative displacement vector and the vector of slippage (inelastic displacement).

The elastic stress (the force per unit area), $\boldsymbol{f}_u$, in a point of a block bottom at time t, is defined by

$$\boldsymbol{f}_u = K_u\,(\Delta \boldsymbol{r}_u - \delta \boldsymbol{r}_u) \qquad (2.1)$$

where $\Delta \boldsymbol{r}_u$ and $\delta \boldsymbol{r}_u$ are, respectively, the block displacement vector relative to the underlying medium and the inelastic displacement vector in the point at the time t.

The evolution of the inelastic displacement in the point is described by the equation

$$\frac{d\delta \boldsymbol{r}_u}{dt} = W_u \boldsymbol{f}_u. \qquad (2.2)$$

The coefficients K_u and W_u in (2.1) and (2.2) can differ for different blocks.

At time t, in some point of a fault zone separating two blocks the elastic stress, $\boldsymbol{f}$, along the fault zone is defined by

$$f = K(\Delta \boldsymbol{r} - \delta \boldsymbol{r}) \tag{2.3}$$

where $\Delta \boldsymbol{r}$ and $\delta \boldsymbol{r}$ are, respectively, the vector of relative displacement of the blocks, along the fault zone, and the inelastic displacement vector along the fault zone, in the point at the time t.

The evolution of the inelastic displacement, $\delta \boldsymbol{r}$, in the point is described by

$$\frac{d\delta \boldsymbol{r}}{dt} = W\boldsymbol{f}. \tag{2.4}$$

The coefficients K and W in (2.3) and (2.4) are, respectively, proportional to the shear modulus and inversely proportional to the viscous coefficient of the fault zone. The values of K and W can differ for different faults.

The reaction force is normal to the fault zone and its size, per unit area, is

$$|p_0| = |f_1 \text{ tg } \alpha| \tag{2.5}$$

where f_1 is a component of the elastic stress, $\boldsymbol{f}$, normal to the fault on the upper plane, and α is a dip angle of the fault zone. The value of p_0 is positive in the case of extension and negative in the case of compression, respectively.

2.4. *Scheme of simulation*

The formulas (2.1)-(2.5) define the stress and the evolution of the inelastic displacements at points of fault zones and of block bottoms. To carry out the numerical simulation of block structure dynamics the discretization of these plane surfaces is needed. The discretization is defined by the parameter ε as follows.

Each fault segment is a trapezium with bases a and b and height $h = H / \sin \alpha$ where H is the thickness of the layer, and α is the dip angle of the fault zone. If we define

$$n_1 = \text{ENTIRE}\,(h/\varepsilon) + 1$$

and

$$n_2 = \text{ENTIRE}\,(\max(a,b)/\varepsilon) + 1,$$

the trapezium is divided into $n_1 n_2$ small trapeziums by two groups of segments inside it: $n_1 - 1$ segments, parallel to the trapezium bases and spaced at intervals h/n_1, and $n_2 - 1$ segments connecting the points spaced by intervals of a/n_2 and b/n_2, respectively, on the two bases. The small trapeziums obtained in such a way are called «cells». The relative displacement of the blocks $\Delta \boldsymbol{r}$ and the inelastic displacement $\delta \boldsymbol{r}$ in (2.3) are supposed to be the same for all the points of a cell.

Bottom of blocks are polygons; they are divided before discretization into trapeziums (triangles) by segments passing through its vertices. These trapeziums (triangles) are discretized in the same way as in the case of fault segments.

The state of the block structure is considered at discrete time $t_1 = t_0 + i\Delta t\,(i = 1, 2, ...)$, where t_0 is the initial time. The transition from the state at time t_i to the state at time t_{i+1} is made as follows:

i) New values of the inelastic displacements in all cells are calculated from eqs. (2.2) and (2.4).

ii) The absolute displacements and rotations at t_{i+1} are calculated for the boundary blocks and the underlying medium.

iii) The components of the translation vectors of the blocks and their rotations about the geometrical centers of the bottoms are determined under the condition that the total force and the total force moment, applied to each block, are equal to zero. This is the condition of quasi-static equilibrium of the system and at the same time the condition of minimum energy.

2.5. *Earthquake and creep*

Earthquakes are simulated in accordance with the dry friction model. Let us introduce the quantity

$$\kappa = \frac{|f|}{P - p_0} \tag{2.6}$$

where f is the elastic stress given by (2.3); P is a parameter of the model which is assumed to be equal for all the faults and can be interpreted as the difference between the lithostatic (due to gravity) and the hydrostatic pressure, and p_0 is the reaction force per unit area given by (2.5). The value of P reflects the average effective pressure in fault zones, and the difference $P - p_0$ is the actual pressure for each cell.

For each fault the following three values of κ are considered

$$B > H_f \geq H_s.$$

Let us assume that the initial conditions for the numerical simulation of block structure dynamics satisfy the inequality $\kappa < B$ for all cells of the fault segments. If at t_i in any cell of a fault segment the value of κ reaches the level B, a failure («earthquake») occurs. The failure is such an abrupt change of the inelastic displacements $\delta \boldsymbol{r}$ in the cell that the value of κ is reduced to the level H_f.

After calculating the new values of the inelastic displacements for all the failed cells, step (iii) of the scheme of simulation is repeated with the same values of the absolute displacements and rotations of the boundary blocks and the underlying medium. If $\kappa > B$ for some cell(s) of the fault segments, the procedure given above is repeated for this cell(s). Otherwise the state of the block structure at time t_{i+1} is determined in the ordinary way.

The cells belonging to a connected set of fault segments in which failure occurs at the same time form a single earthquake.

It is assumed that immediately after the earthquake the cells in which failure has occurred are in the creep state. This means that, for these cells, in eq. (2.4), which describes the evolution of inelastic displacement, the parameter W_s ($W_s > W$) is used instead of W; and that W_s can differ for different faults. After the earthquake, the cell is in the creep state as long as $\kappa > H_s$, when $\kappa \leq H_s$; the cell returns to the normal state and henceforth, for this cell, the parameter W is used in (2.4).

3. Dynamics of synthetic seismicity

3.1. *Clustering of earthquakes in the model*

The possibility of earthquakes clustering in the synthetic catalog was considered by Gasilov *et al.* (1995) and by Maksimov and Soloviev (1996). It is of vital importance to determine whether clustering is caused by the specific tectonic features of a region or is a general phenomenon for a wide variety of neotectonic conditions which reflects the general features of systems of interacting with blocks of the seismogenic lithosphere. The results obtained show that the phenomenon of clustering is observed for a structure consisting of four identical square blocks when a simple movement of one boundary is prescribed (fig. 2), and this clustering of earthquakes in a synthetic catalog arising from modeling of dynamics of a simple block structure favours the second hypothesis.

The block structure in fig. 2 consists of four blocks whose common parts with the upper plane are squares with a side of 50 km. The

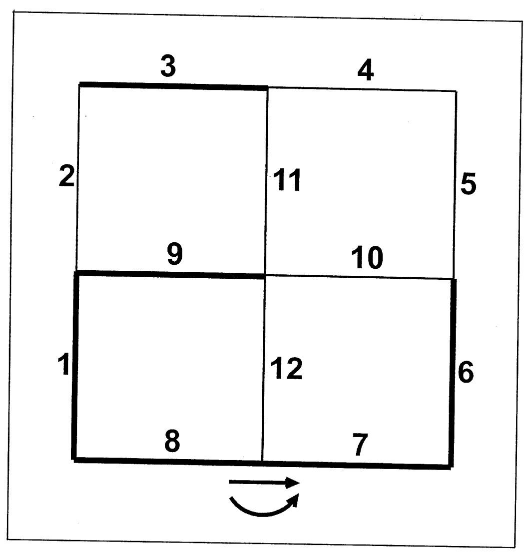

Fig. 2. The block structure (the numbers of fault segments are indicated) for which clustering is studied.

thickness of the layer is $H = 20$ km. All fault zones have the same (85°) angle of dip. It is assumed that the boundary consisting of the fault segments numbered 8 and 7 moves translationally with the components of velocity $V_x = 20$ cm and $V_y = 0$ cm and rotates around the point $X = 50$ km, $Y = 0$ (the common point of segments 8 and 7 on the upper plane) at an angular velocity of 10^{-6} radians. The other parts of the structure boundary and the underlying medium do not move.

For all faults the parameters in (2.3)-(2.4) and the levels for κ (2.6) have the same values: $K = 1$ bars/cm; $W = 0.05$ cm/bars; $W_s = 1$ cm/bars; $B = 0.1$; $H_f = 0.085$; $H_s = 0.07$. For all blocks the parameters in (2.1)-(2.2) also have the same values: $K_u = 1$ bars/cm; $W_u = 0.05$ cm/bars. The parameter P in (2.6) is equal to 2 Kbars. The discretization is defined by the following values: $\varepsilon = 5$ km, $\Delta t = 0.01$.

The numerical simulation was made with zero initial conditions (zero displacement of

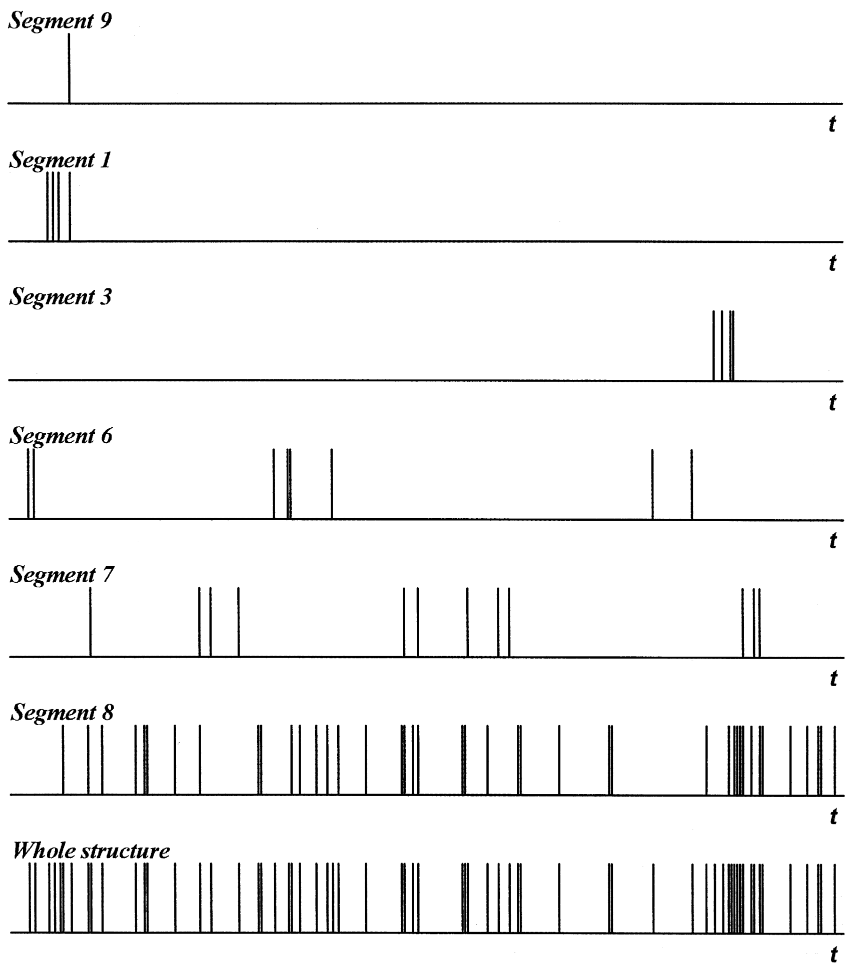

Fig. 3. Clustering of earthquakes: the times of earthquakes (vertical lines) for individual fault segments and for the whole structure for a time interval of 3 units.

the boundary blocks and the underlying medium and zero inelastic displacements for all cells). The occurrence times of earthquakes (vertical lines) are shown in fig. 3 for individual fault segments and for the whole structure during the time interval of 3 units starting at $t = 480$.

Earthquakes occur on six fault segments. Segment 9 has one earthquake only for the period under consideration. Clustering of earthquakes appears clearly on fault segments 1, 3, 6 and 7. Segment 8 has the largest number of earthquakes. Here the clustering appears weaker: the groups of earthquakes are spread along the time axis. The picture for the whole structure looks similar, but groups of earthquakes can be identified.

Clustering for other time intervals is not substantially different from that presented in fig. 3.

3.2. *Dependence of synthetic seismicity on structure fragmentation and boundary movements*

Fragmentation of the media is generally regarded as a factor which reduces the occurrence of strong earthquakes. We demonstrate here, that this is not necessarily the case.

Seismic observations show that features of the seismic process may differ for different regions (see, for example, Hattori, 1974; Kronrod, 1984). It is reasonable to suggest that this difference is due, among other factors, to varying tectonic structure of the regions and the main tectonic movements determining the lithosphere dynamics. Laboratory studies show specifically that the differences are largely controlled by the rate of fracturing and heterogeneity of the medium and also by the type of predominant tectonic movements (Mogi, 1962; Shamina *et al.*, 1980; Sherman *et al.*, 1983).

If a single factor is considered, it is difficult to detect its impact on the features of the seismic process by using real seismic observations, because earthquakes are affected by a number of factors some of which could be stronger than the one under consideration. This can be overcome by numerically modelling the earthquake-generating process and studying the synthetic earthquake catalog obtained (see, for example, Allegre *et al.*, 1995; Newman *et al.*, 1995; Shaw *et al.*, 1992; Turcotte, 1992).

The block model is used to simulate seismicity for three groups of structures with increasing structure fragmentation within each group and for two types of boundary movements.

The faults in these structures on the upper plane are shown in fig. 4. One structure (BS1) belongs to all groups. Its faults on the upper plane form a square with a side of 320 km divided into four smaller squares. Two other structures of the first (BS12, BS13), second (BS22, BS23), and third (BS32, BS33) group are obtained from BS1 by subdivision in the self-similar way (Bariere and Turcotte, 1994).

The thickness of the layer is $H = 20$ km for all structures.

The values of the parameters in (2.1)-(2.2) for all blocks are $K_u = 1$ bar/cm and $W_u = 0.05$ cm/bars.

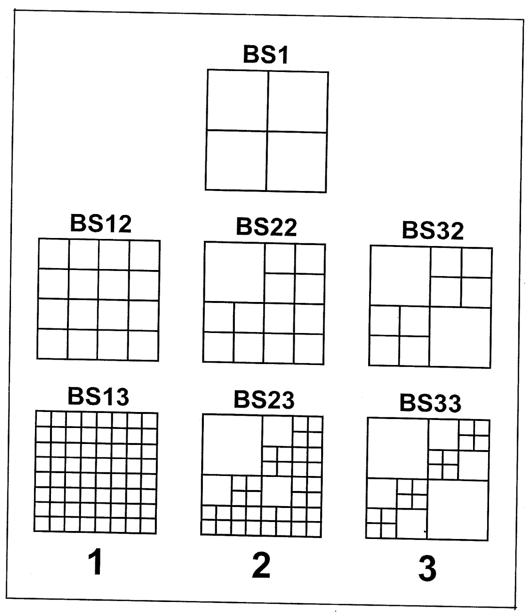

Fig. 4. Schemes on the upper plane of faults of block structures under consideration: 1 = first group (BS1, BS12, BS13); 2 = second group (BS1, BS22, BS23); 3 = third group (BS1, BS32, BS33).

The parameters in (2.3)-(2.4) for the faults are the following: $\alpha = 85°$ (dip angle); $K = 1$ bar/cm; $W = 0.05$ cm/bars; $W_s = 10$ cm/bars. The levels of κ (2.6) are the same for all faults: $B = 0.1$; $H_f = 0.085$; $H_s = 0.07$. The parameter P in (2.6) is 2 Kbars.

The parameters for time and space discretization are, respectively: $\Delta t = 0.001$, $\varepsilon = 5$ km.

The medium underlying all blocks of the structures does not move.

Two types of boundary movement are considered (fig. 5a,b).

The first type is a translational movement at a velocity of 10 cm per unit non-dimensional time. The directions of the velocity vectors are shown in fig. 5a. The angle between the velocity vector and the proper side of the square outlining a structure is 10°.

The second type involves a translational movement and a rotation (fig. 5b). Two boundaries move translationally at a velocity of 10 cm per unit non-dimensional time. The velocity vectors are parallel to the respective sides of the square that encloses the structure. The other two boundaries rotate about the centers of the respective sides of the square at an angular velocity of $-0.625\ 10^{-6}$ radians per unit non-dimensional time.

Numerical simulation of dynamics for all the block structures under consideration was carried out for a period of 200 non-dimensional time units starting from the initial zero condition with both types of boundary movement.

As a result, synthetic earthquake catalogs were obtained. The magnitude of the earthquake is calculated from

$$M = 0.98 \log S + 3.93 \tag{3.1}$$

where S is the sum of the areas of the cells (in km^2) forming the earthquake. The constants in (3.1) are specified in accordance with Utsu and Seki (1954).

The cumulative frequency-magnitude plots for the synthetic catalogs obtained for the first type of boundary movement are presented in fig. 6. The shape of the plots is in accordance with the Gutenberg-Richter law for observed seismicity: the logarithm of the number of earthquakes is a linear function of magnitude.

The cumulative frequency-magnitude plots for the synthetic catalogs for the second type of boundary movement are presented in fig. 7.

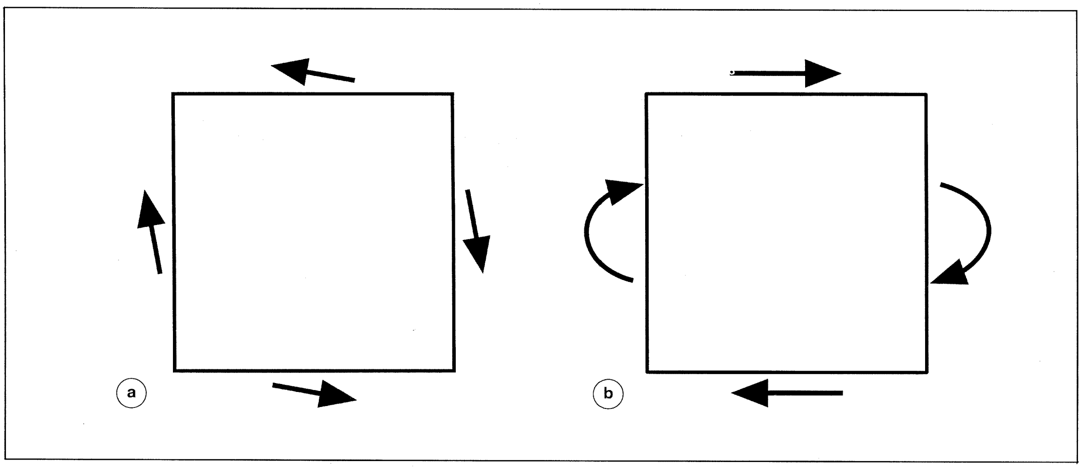

Fig. 5a,b. Types of boundary movement considered (the arrows show the vectors of boundary velocities): a) first type, all velocities are 10 cm, the angle between the velocity vectors and the relevant boundary faults is 10°; b) second type, the velocities of translational movement is 10 cm, the angular velocity is $-0.625\ 10^{-6}$ radians.

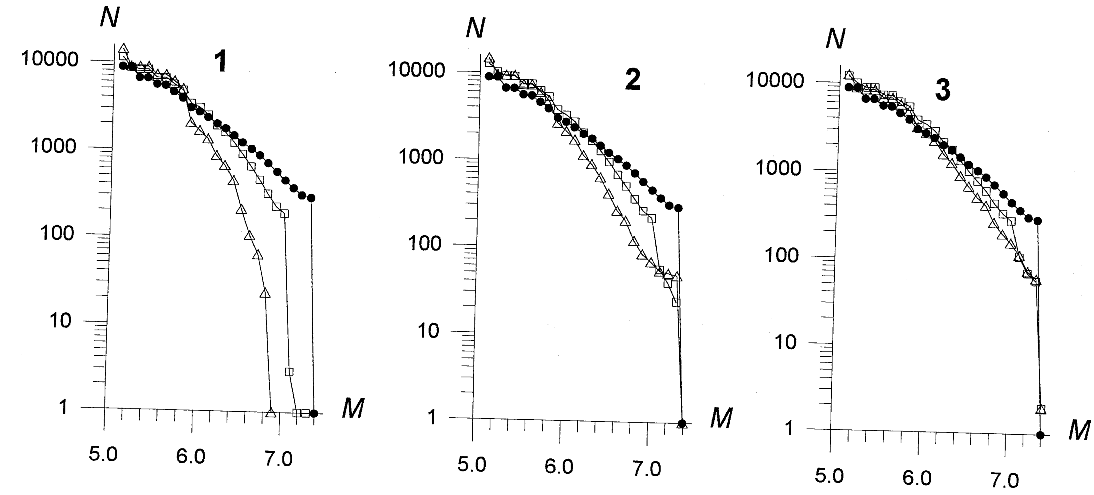

Fig. 6. Cumulative frequency-magnitude relations for the synthetic catalogs obtained with the boundary movement without rotation. Dots mark the curves corresponding to BS1, squares to BS12, BS22, and BS32, triangles to BS13, BS23, and BS33. (1) corresponds to the first group of structures, (2) to the second, (3) to the third.

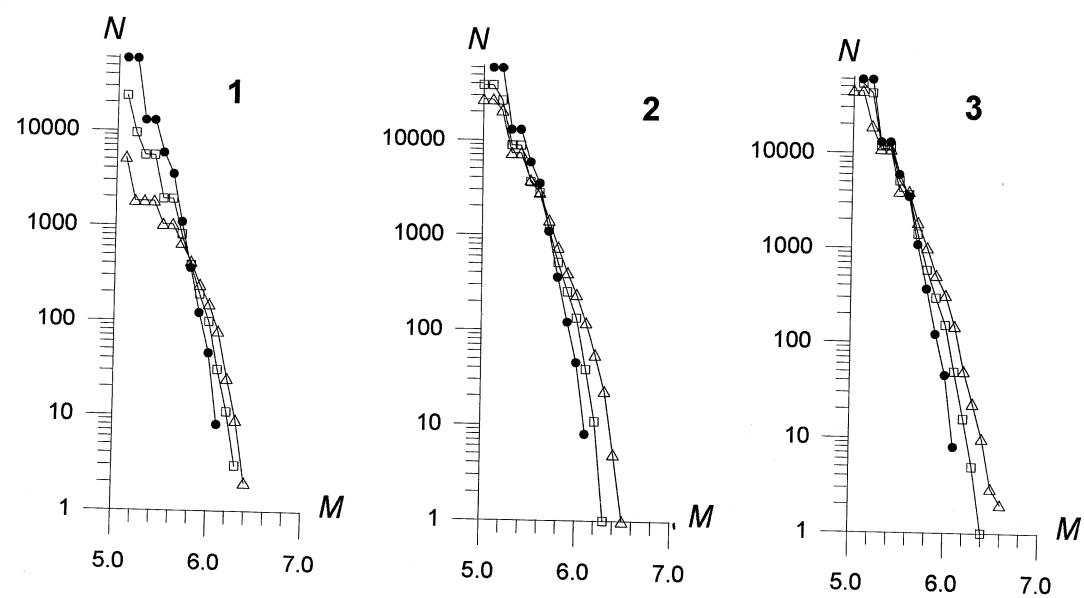

Fig. 7. Cumulative frequency-magnitude relations for synthetic catalogs obtained with boundary movement with rotation. Notation is the same as in fig. 6.

Figure 6 shows that in the case of non-rotational boundary movement the cumulative frequency-magnitude plots vary similarly within each group of self-similar structures, when structure fragmentation increases. The following variation is observed: the total number of events and the number of small events increase; the number of large events decreases; the *b*-value increases. The largest difference between the plots for different structures appears in group 1 (structures BS1, BS12, BS13).

When boundary movement with rotation is considered (fig. 7), the cumulative frequency-magnitude plots also vary similarly in different groups of structures, but when structure fragmentation increases, the variation in each group is *opposite* (compared to non-rotational boundary movement): the total number of events and the number of small events decrease; the number of large events increases; the *b*-value decreases. For this type of boundary movement, the largest difference between the plots for different structures is again in the first group.

3.3. *Dependence of synthetic seismicity on the movements of the boundaries and of the underlying medium*

The seismic activity of a fault depends on the rate of relative tectonic movements on it, these movements being interrelated in a system of faults. Therefore, the spatial distribution of seismicity can be used not only to compare activity on different faults, but also to reconstruct block motion. It is even possible to formulate the inverse problem: reconstruct block motions using the observed distribution of epicentres and other seismicity features.

Such reconstruction becomes possible by using the model of block structure dynamics. The numerical experiments were carried out for the model of lithosphere dynamics of the Near East region (Sobolev *et al.*, 1996) and for the model of the Vrancea region (Soloviev *et al.*, 1996; Panza *et al.*, 1997; Vorobieva and Soloviev, 1997) showing that the spatial distribution of epicenters is sensitive to the direction of block motion.

The results below were obtained for the block structure approximating a morphostructural zoning scheme of the Western Alps. The scheme of morphostructural zoning for the Western Alps (Cisternas *et al.*, 1985) was used earlier as a basis for developing a block structure of that region (Gabrielov *et al.*, 1994; Gasilov *et al.*, 1995). The structure had the same degree of detail as the source map of morphostructural zoning. Low rank lineaments were eliminated from the map to yield a rough morphostructural scheme and a block structure in which the dependence of simulated seismicity features on the boundary movement is

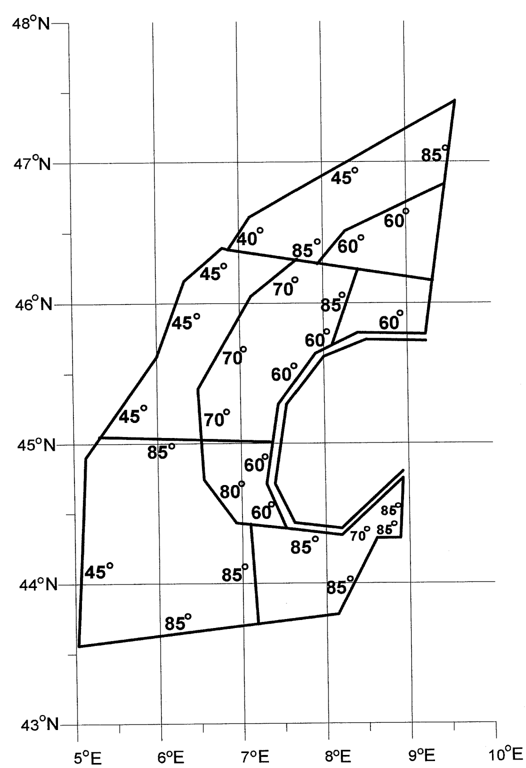

Fig. 8. Block structure approximating a morphostructural zonation of the Western Alps, the dip angles of the fault zones are given near of respective faults.

studied. The scheme of the faults of the block structure on the upper plane is shown in fig. 8.

The following values were ascribed to the parameters of the block structure. The depth of the layer is $H = 30$ km. The parameter P in (2.6) is 2 Kbars. The time and space discretizations are defined by $\Delta t = 0.001$ and $\varepsilon = 5$ km. The parameters in (2.3)-(2.4) and the levels for κ (2.6) are the same for all faults: $K = 1$ bars/cm; $W = 0.05$ cm/bars; $W_s = 10$ cm/bars; $B = 0.1$; $H_f = 0.085$, $H_s = 0.07$. The parameters in (2.1) and (2.2) are also the same for all blocks: $K_u = 1$ bars/cm; $W_u = 0.05$ cm/bars. The dip angles of the fault zones are shown in fig. 8.

The Western Alps is a continental collision zone within the Mediterranean orogenic mobile belt. The regional stress field is controlled by the interaction between the Apennine and Western European plates. According to plate tectonics, the Apennine plate moves northwest, causing compression in the Western Alps (McKenzie, 1970). The part of the boundary shown as a double line in fig. 8 (this part of the

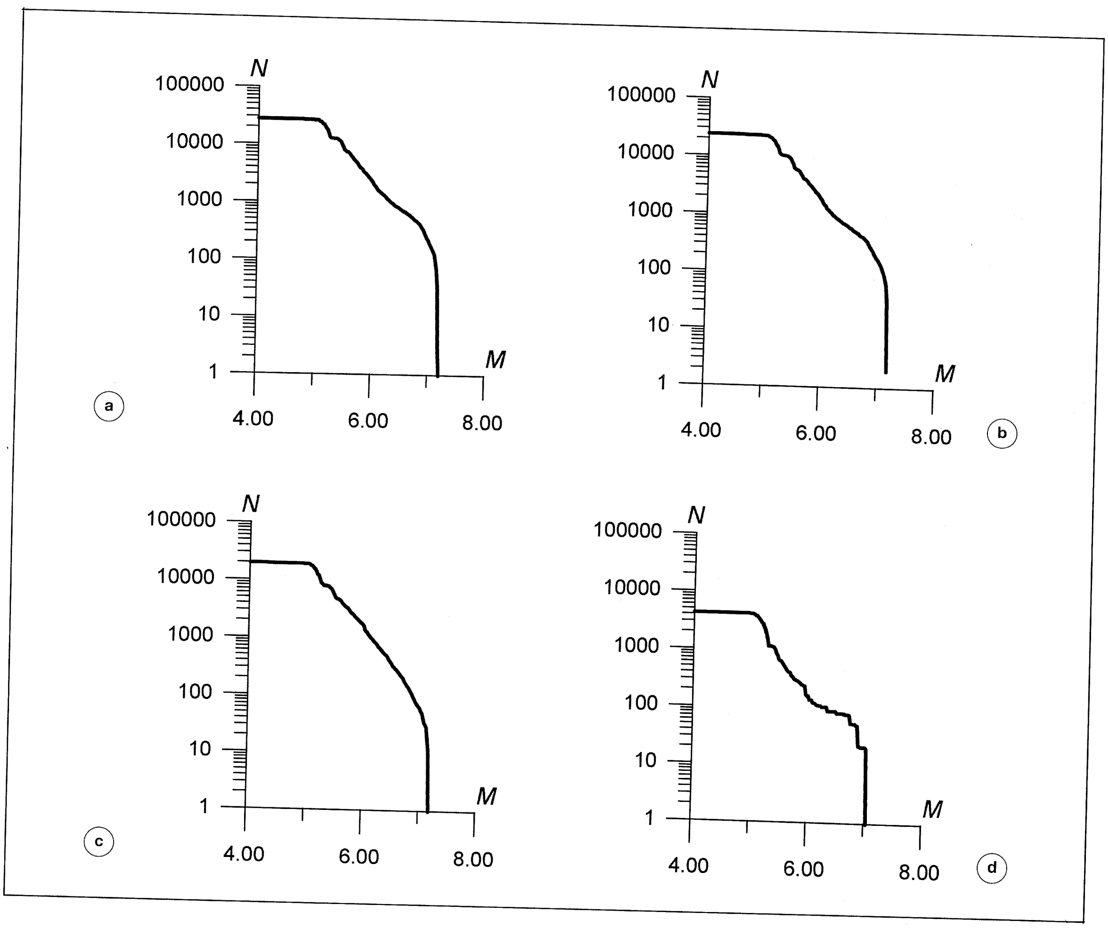

Fig. 9a-d. Cumulative frequency-magnitude relations for synthetic catalogs obtained in a block model approximating the rough map of morphostructural zoning for Western Alps with different angles between the vector of the boundary movement velocity and the north-oriented meridian: a) 30°; b) 45°; c) 60°; d) 90°.

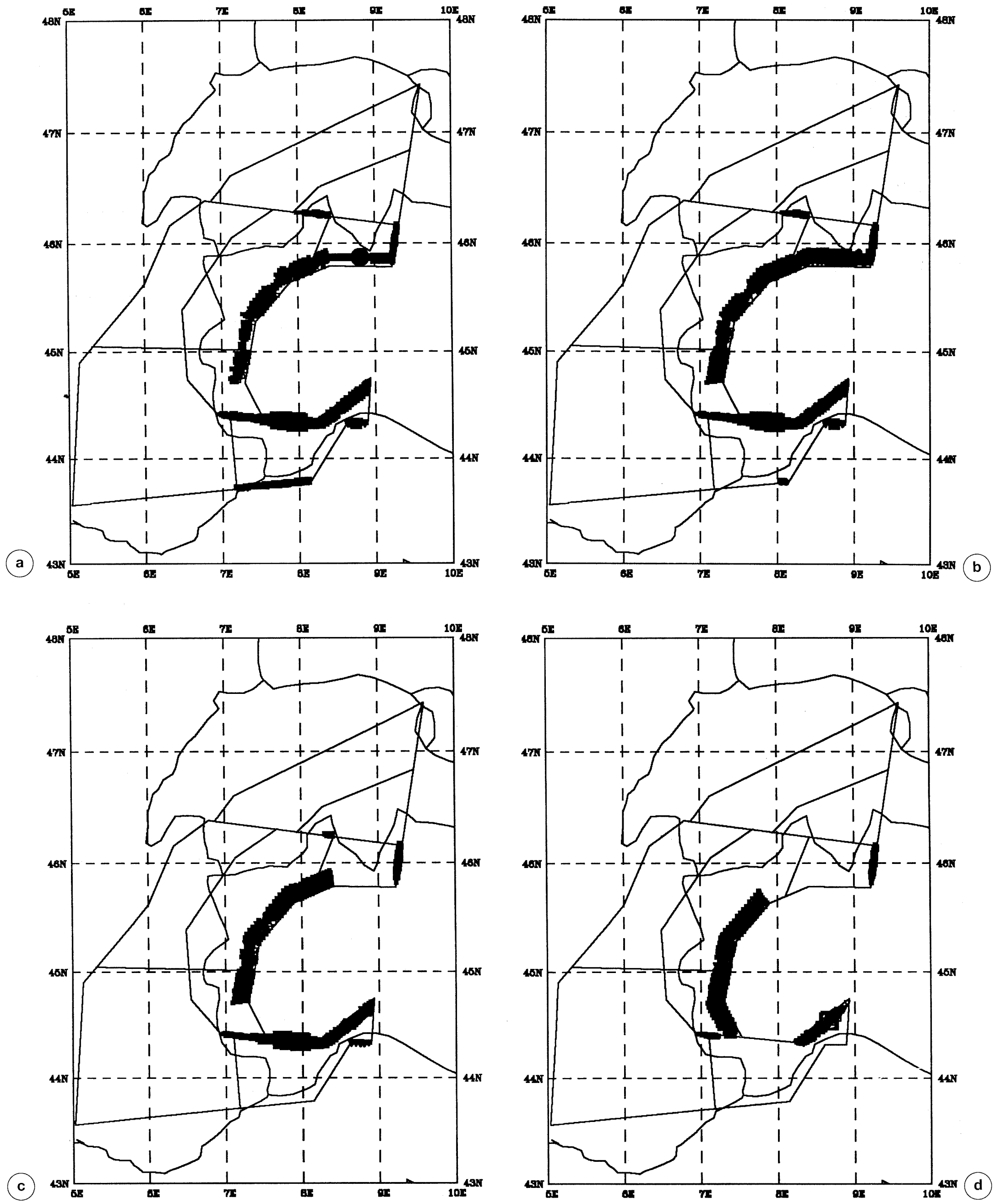

Fig. 10a-d. Maps of synthetic seismicity obtained in a block model approximating the rough map of morphostructural zoning for Western Alps with different angles between the velocity vector of the boundary movement and the north-oriented meridian: a) 30°; b) 45°; c) 60°; d) 90°.

boundary corresponds to the boundary between the Alps and the Apennines) moves translationally, while other parts of the boundary, as well as the underlying medium, do not move. The velocity of boundary movement is 10 cm. The angle between the velocity vector and the north-looking meridian varied between 30° and 90°.

The synthetic earthquake catalogs were obtained as a result of this block structure dynamics simulation, for the period of 200 units of non-dimensional time starting from the initial zero condition (zero displacement of boundary blocks and the underlying medium and zero inelastic displacements for all cells). The magnitude of earthquakes was calculated by (3.1). The cumulative frequency-magnitude plots for the synthetic catalogs are presented in fig. 9a-d.

It follows from fig. 9a-d that the frequency-magnitude plot depends on the direction of the boundary movement velocity vector. The total number of events in the synthetic catalog decreases when the angle between the velocity vector and the north increases from 30° to 90°: 27210 (30°); 23630 (45°); 19521 (60°); 4255 (90°). The shape of the curve for 90° differs significantly from that of the other curves. This curve reflects an abnormal abundance of large earthquakes that can be interpreted as the presence of a «characteristic earthquake».

The spatial distribution of epicenters in the synthetic earthquake catalog also depends on the direction of the boundary movement velocity vector. This is illustrated by fig. 10a-d. One can therefore hope to obtain in the model a spatial distribution of epicenters close to that observed in the Western Alps by specifying a suitable movement of the boundaries and the underlying medium.

3.4. *Dependence of the synthetic earthquake catalog on space discretization*

As mentioned above, the space discretization was made with $\varepsilon = 5$ km for the Western Alps block model. Numerical simulation was carried out for this structure with different values of ε (the variant with an angle of 45° between the velocity vector of boundary movement and the north was alone examined).

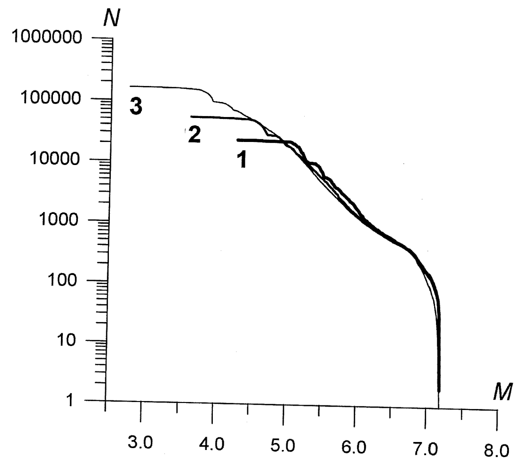

Fig. 11. Cumulative frequency-of-occurrence plots for the synthetic catalogs with different space discretization: $\varepsilon = 5$ km (1); $\varepsilon = 2.5$ km (2); $\varepsilon = 1$ km (1).

The values $\varepsilon = 2.5$ and 1 km were considered, in addition to $\varepsilon = 5$ km. The cumulative frequency-magnitude plots (fig. 11) show that the decrease of ε has nearly no effect of decreasing the number of earthquakes in the magnitude range corresponding to the previous value of ε. The total number of earthquakes in the catalog increases due to extension of the magnitude range to smaller magnitudes. The b-value does not change as ε decreases.

It follows from (3.1) that the minimum magnitude in the synthetic catalog must be about 3.9, 4.7, and 5.3 for the values $\varepsilon = 1$, 2.5, and 5 km, respectively. These minimum magnitudes are reflected in the behaviour of the curves in fig. 11.

4. Conclusions

The clustering of earthquakes which was found in the model allows clustering to be modelled in specific seismic regions. In particular, the dependence of clustering on block structure geometry and the model parameters can be ascertained.

The results described above show that the features of a catalog obtained by numerical simulation depend on block structure geometry and boundary movement. The character of the dependence on the geometry changes dramatically with the other type of boundary movement. Note that for the boundary movement with rotation the dependence of the above seismicity characteristics on structure fragmentation *is in contradiction with the currently accepted view*.

The structures considered have an artificial geometry and present no exact analogy with tectonic structure of any real seismic region, in contrast to the structures studied by Gabrielov *et al.* (1994), Sobolev *et al.* (1996) and Panza *et al.* (1997). Nevertheless, the dependence of seismicity features on tectonic structure fragmentation was detected in some seismic regions (Hattori, 1974; Kronrod, 1984). Note that the slope (b-value) of the Gutenberg-Richter curve obtained for non-rotational boundary movement (fig. 6) is close to that for the actually observed seismicity (~ 1). For the boundary movement with rotation (fig. 7) the b-value is larger. One is thus confronted with the problem of analysis of seismicity in different seismic regions in order to find similar features in the dependence of seismicity on the fragmentation of tectonic structure.

The dependence of the features of the synthetic earthquake catalog on the prescribed movements of block structure boundaries and of the underlying medium is found for the block structure models. This reflects the fact that the seismic activity of a fault depends on the rate of relative tectonic movements along it, and these movements are caused by movements of the blocks forming the structure. Therefore, the spatial distribution of seismicity can be used not only to compare activity on different faults, but also to reconstruct block motion. It is even possible to formulate the inverse problem: *reconstruct block motions using the observed distribution of epicentres and other seismicity features*. Such reconstruction becomes possible using the model of block structure dynamics. The numerical experiments carried out by varying the values of model parameters show that the spatial distribution of epicenters is sensitive to the direction of block motion. The results of the experiments allow us to state that it is possible to use this procedure of block structure dynamics modelling to reconstruct block motions using the observed distribution of epicentres and other seismicity features.

The values of the model parameters for which some similarity between the synthetic and the real catalogs is achieved can be useful for estimating the rates of tectonic movements and the physical parameters involved in the dynamic processes in the fault zones.

The results of the experiments in varying the parameter ε determining the model space discretization show that a synthetic earthquake catalog for which the linear part of the frequency-of-occurrence plot (fig. 11) spans as much as 3 magnitude units can be obtained in the block model. We calculated the total strain energy released through the earthquakes for the synthetic catalogs obtained. As shown in Keilis-Borok *et al.* (1997) the energy released through an earthquake is proportional in the model to the sum S of the areas of the cells forming the earthquake. Total energy was found not to change as ε decreases.

The results listed above show that modelling of block structure dynamics is a useful tool to study the relations between fault geometry and block movements and earthquake flow, including premonitory seismicity patterns, to test the existing earthquake prediction algorithms, and to develop new ones. This is confirmed by the results of application of the intermediate-term prediction algorithm $M8$ to the synthetic earthquake catalog (Gabrielov *et al.*, 1994).

Acknowledgements

This work was supported by U.S. National Science Foundation (grant EAR 94-23818) and by the Russian Foundation for Basic Research (grants RFFI 96-05-65710 and RFFI 97-05-65802).

REFERENCES

ALLEGRE, C.J., J.-L. LE MOUEL, H.D. CHAU and C. NARTEAU (1995): Scaling organization of fracture tectonics (SOFT) and earthquake mechanism, *Phys. Earth. Planet. Inter.*, **92**, 215-233.

BARIERE, B. and D.L. TURCOTTE (1994): Seismicity and self-organized criticality, *Phys. Rev. E*, **49** (2), 1151-1160.

CAPUTO, M., V.I. KEILIS-BOROK, T.L. KRONROD, G.M. MOLCHAN, G.F. PANZA, A. PIVA, V.M. PODGAETSKAJA and D. POSTPISCHL (1973): Models of earthquake occurrence and isoseismals in Italy, *Ann. Geofis.*, **26** (2-3), 421-444.

CAPUTO, M., V.I. KEILIS-BOROK, T.L. KRONROD, G.M. MOLCHAN, G.F. PANZA, A. PIVA, V.M. PODGAETSKAJA and D. POSTPISCHL (1974): The estimation of seismic risk for Central Italy, *Ann. Geofis.*, **27**. 349-365.

CAPUTO, M., V. KEILIS-BOROK, E. OFICEROVA, E. RANZMAN, I. ROTWAIN and A. SOLOVIEFF (1980): Pattern recognition of earthquake-prone areas in Italy, *Phys. Earth Planet. Inter.*, **21**, 305-320.

CISTERNAS, A., P. GODEFROY, A. GVISHIANI, A.I. GORSHKOV, V. KOSOBOKOV, M. LAMBERT, E. RANZMAN, J. SALLANTIN, H. SALDANO, A. SOLOVIEV and C. WEBER (1985): A dual approach to recognition of earthquake prone areas in the Western Alps, *Ann. Geophysicae*, **3** (2), 249-270.

GABRIELOV, A.M., T.A. LEVSHINA and I.M. ROTWAIN (1990): Block model of earthquake sequence, *Phys. Earth Planet. Inter.*, **61** (1-2), 18-28.

GABRIELOV, A., V. KOSSOBOKOV and A. SOLOVIEV (1994): Numerical simulation of block structure dynamics, in *Seismicity and Related Processes in the Environment*, Research and Coordinating Centre for Seismology and Engineering, vol. 1.M., 22-32.

GASILOV, V., V. MAKSIMOV, V. KOSSOBOKOV, A. PROZOROV and A. SOLOVIEV (1995): Numerical simulation of block structure dynamics. II. Examples, in *Third Workshop on Non-Linear Dynamics and Earthquake Prediction, 6-17 November 1995, Trieste*, ICTP, H4.SMR/879-3, pp. 48.

GORSHKOV, A.I. and A.A. SOLOVIEV (1996): The Western Alps: numerical modelling of block structure and seismicity, in *XXV General Assembly of the European Seismological Commission, September 9-14, 1996, Reykjavik, Iceland*, abstracts 66.

HATTORI, S. (1974): Regional distribution of *b*-value in the world, *Bull. Int. Inst. Seismol. Earth Eng.*, **12**, 39-58.

KEILIS-BOROK, V.I. (Editor) (1990): Intermediate-term earthquake prediction: models, algorithms, woldwide tests, *Phys. Earth Planet. Inter.*, **61** (1-2), special issue.

KEILIS-BOROK, V.I. (1996): Intermediate-term earthquake prediction, *Proc. Nat. Acad. Sci. USA*, **93**, 3748-3755.

KEILIS-BOROK, V.I. and L.N. MALINOVSKAYA (1964): One regularity in the occurrence of strong earthquake, *J. Geophys. Res.*, **69**, 3019-3024.

KEILIS-BOROK, V.I., I.M. ROTWAIN and A.A. SOLOVIEV (1997): Numerical modeling of block structure dynamics: dependence of a synthetic earthquake flow on the structure separateness and boundary movements, *J. Seism.* (in press).

KRONROD, T.L. (1984): Seismicity parameters of the main regions of the high seismic activity, in *Logical and Computational Methods in Seismology*, edited by V.I. KEILIS-BOROK and A.L. LEVSHIN (Nauka, Moscow), 36-57; *Comput. Seismol.*, No. 17 (in Russian).

MAKSIMOV, V.I. and A.A. SOLOVIEV (1996): Clustering of earthquakes in block model of lithosphere dynamics, in *Modern Problems of Seismicity and Earth Dynamics*, edited by V.I. KEILIS-BOROK and A.L. MOLCHAN (Nauka, Moscow), 148-152; *Comput. Seismol.*, No. 28 (in Russian).

MCKENZIE, D.P. (1970): Plate tectonics of the Mediterranean region, *Nature*, **226**, 239-243.

MOGI, K. (1962): Magnitude-frequency relation for elastic shocks accompanying fractures of various materials and some related problems in earthquakes, *Bull. Earthq. Inst. Tokyo Univ.*, **40**, 831-853.

MOLCHAN, G.M., O.E. DMITRIEVA, I.M. ROTWAIN and J. DEWEY (1990): Statistical analysis of the results of earthquake prediction, based on bursts of aftershocks, *Phys. Earth Planet. Inter.*, **61** (1-2), 128-139.

NEWMAN, W.I., D.L. TURCOTTE and A.M. GABRIELOV (1995): Log-periodic behaviour of a hierarchical failure model with application to precursory seismic activation, *Phys. Rev. E.*, **52**, 4827-4835.

PANZA, G.F., A.A. SOLOVIEV and I.A. VOROBIEVA (1997): Numerical modelling of block-structure dynamics: application to the Vrancea region, *Pageoph*, **149**, 313-336.

ROTWAIN, I. and O. NOVIKOVA (1997): Performance of the earthquake prediction algorithm CN in 21 regions of the world, in *Fourth Workshop on Non-Linear Dynamics and Earthquake Prediction, 6-24 October 1997, Trieste*, ICTP, H4.SMR/1011-21, pp. 19.

ROTWAIN, I., V. KEILIS-BOROK and L. BOTVINA (1997): Premonitory transformation of steel fracturing and seismicity, *Phys. Earth Planet. Inter.*, **101**, 61-71.

SHAMINA, O.G., V.A. BUDNIKOV, S.D. VINOGRADOV, M.P. VOLAROVICH and I.S. TOMASHEVSKAYA (1980): Laboratory experiments on the physics of the earthquake source, in *Physical Processes in Earthquake Sources* (Nauka, Moscow), 56-68 (in Russian).

SHAW, B.E., J.M. CARLSON and J.S. LANGER (1992): Patterns of seismic activity preceding large earthquakes, *J. Geophys. Res.*, **97**, 479-488.

SHERMAN, S.I., S.A. BORNIAKOV and V.YU. BUDDO (1983): *Areas of Dynamic Effects of Faults* (Nauka, Novosibirsk), pp. 111 (in Russian).

SOBOLEV, P.O., A.A. SOLOVIEV and I.M. ROTWAIN (1996): Modelling of lithosphere dynamics and seismicity for the Near East region, in *Modern Problems of Seismicity and Earth Dynamics*, edited by V.I. KEILIS-BOROK and G.M. MOLCHAN (Nauka, Moscow), 131-147; *Comput. Seismol.*, No. 28 (in Russian).

SOLOVIEV, A.A. (1995): Modeling of block structure dynamics and seismicity, in *European Seismological Commission, XXIV General Assembly, 1994 September 19-24, Athens, Greece, Proceedings and Activity Re-*

port 1992-1994, University of Athens, Faculty of Sciences, Subfaculty of Geosciences, Department of Geophysics and Geothermy, vol. 3, 1258-1267.

SOLOVIEV, A.A., I.A. VOROBIEVA and G.F. PANZA (1996): Reconstruction of lithosphere motions using numerical modelling of block structure dynamics: application to the Vrancea region, Trieste, ICTP Preprint IC/96/244, pp. 28.

TURCOTTE, D.L. (1992): *Fractals and Chaos in Geology and Geophysics* (Cambridge University Press), pp. 221.

UTSU, T. and A. SEKI (1954): A relation between the area of aftershock region and the energy of main shock, *J. Seism. Soc. Japan*, **7**, 233-240.

VOROBIEVA, I.A. (1997): Prediction of a next large earthquake, in *Fourth Workshop on Non-Linear Dynamics and Earthquake Prediction, 6-24 October 1997, Trieste*, ICTP, H4.SMR/1011-29, pp. 16.

VOROBIEVA, I.A. and A.A. SOLOVIEV (1997): Connection between space distribution of earthquake epicenters and movement of lithosphere blocks, *Doklady of Russian Ac. Sci.* (in Russian), (in press).